

# Dissipation and spontaneous symmetry breaking in brain dynamics

Walter J Freeman<sup>1</sup> and Giuseppe Vitiello<sup>2</sup>

<sup>1</sup> Department of Molecular and Cell Biology, University of California, Berkeley, CA 94720-3206, USA

<sup>2</sup> Dipartimento di Matematica e Informatica, Università di Salerno, and Istituto Nazionale di Fisica Nucleare, Gruppo Collegato di Salerno, I-84100 Salerno, Italy

E-mail: [dfreeman@berkeley.edu](mailto:dfreeman@berkeley.edu) and [vitiello@sa.infn.it](mailto:vitiello@sa.infn.it)

Received 26 October 2007, in final form 24 January 2008

Published 15 July 2008

Online at [stacks.iop.org/JPhysA/41/304042](http://stacks.iop.org/JPhysA/41/304042)

## Abstract

We compare the predictions of the dissipative quantum model of the brain with neurophysiological data collected from electroencephalograms resulting from high-density arrays fixed on the surfaces of primary sensory and limbic areas of trained rabbits and cats. Functional brain imaging in relation to behavior reveals the formation of coherent domains of synchronized neuronal oscillatory activity and phase transitions predicted by the dissipative model.

PACS numbers: 11.10.-z, 87.85.dm, 11.30.Qc

## 1. Introduction

In his pioneering work in the first half of the 20th century, Lashley was led to the hypothesis of ‘mass action’ in the storage and retrieval of memories in the brain and observed: ‘... Here is the dilemma. Nerve impulses are transmitted ... from cell to cell through definite intercellular connections. Yet, all behavior seems to be determined by masses of excitation ... within general fields of activity, without regard to particular nerve cells ... What sort of nervous organization might be capable of responding to a pattern of excitation without limited specialized path of conduction? The problem is almost universal in the activity of the nervous system’ (pp 302–6 of [1]). Lashley’s finding was confirmed in many subsequent laboratory observations and Pribram then proposed the analogy between the fields of distributed neural activity in the brain and the wave patterns in holograms [2].

Mass action has been confirmed by EEG, by magnetoencephalogram (MEG), functional magnetic resonance imaging (fMRI), positron electron tomography (PET) and single photon emission computed tomography (SPECT). These techniques gave observational access to real-time imaging of ‘patterns of excitation’ and dynamical formation of spatially extended domains of neuronal fields of activity. The neocortex is observed to be characterized by the

exchangeability of its ports of sensory input; its ability to adapt rapidly and flexibly to short- and long-term changes; its reliance on large-scale organization of patterns of neural activity that mediate its perceptual functions; the incredibly small amounts of information entering each port in brief behavioral time frames that support effective and efficient intentional action and perception [3, 4].

None of the following four material agencies which have been proposed to account for the processes involving large populations of neurons, appear to be able to explain the observed cortical activity [5].

- (1) Nonsynaptic transmission is essential for neuromodulation and diffusion of chemical fields of metabolites providing manifestations of widespread coordinated firing. It has been proposed [3] as the mechanism for implementation of volume transmission to answer the question of how broad and diffuse chemical gradients might induce phase locking of neural pulse trains at ms intervals. However, it is too slow to explain the highly textured patterns and their rapid changes [5]. Observations [6] show that cortex indeed jumps abruptly from a receiving state to an active transmitting state. Spatial amplitude modulated (AM) patterns with carrier frequencies in the beta and gamma ranges (12–80 Hz) form during the active state and dissolve as the cortex returns to its receiving state after transmission. These state transitions in cortex form frames of AM patterns in few ms, hold them for 80–120 ms, and repeat them at rates in alpha and theta ranges (3–12 Hz) of EEG [7, 6, 13]. These patterns appear often to extend over spatial domains covering much of the hemisphere in rabbits and cats [12, 6], and over the length of a  $64 \times 1$  linear 19 cm array [8] in human cortex with near zero phase dispersion [13, 14]. Synchronized oscillation of large-scale neuronal assemblies in beta and gamma ranges has been detected in the resting state and in motor task related states of the human brain by MEG [15]. The observed high rates of field modulation are not compatible with mediation of chemical diffusion such as those estimated in studies of spike timing among multiple pulse trains (e.g. [16–18]), of cerebral blood flow using fMRI (e.g. [19, 20]) and of spatial patterns of the distributions of radio-labelled neurotransmitters and neuromodulators as measured with PET, SPECT and optical techniques.
- (2) Electric fields are revealed by the extracellular flow of dendritic current across the resistance of brain tissue [21]. Weak extracellular electric currents have been shown to modulate the firing of neurons *in vitro* and have been postulated as the agency by which neurons are linked together [22]. However, the current densities required *in vivo* to modulate cortical firing exceed by nearly two orders of magnitude those currents that are sustained by extracellular dendritic currents [21, 23].
- (3) Magnetic fields of such intensity which can be measured 4–5 cm above the scalp with MEG are generated by the intracellular current in palisades of dendritic shafts in cortical columns. The earth's far stronger magnetic field can be detected by specialized receptors for navigation in birds and bees [24], leading to the search for magnetic receptors among cortical neurons (e.g. [25, 26]), so far without positive results.
- (4) The combined agency of electric and magnetic fields propagating as radio waves has also been postulated [27]. However, neuronal radio communication is unlikely, owing to the 80:1 disparity between electric permittivity and magnetic permeability of the brain tissue and to the low frequency (<100 Hz) and kilometer wavelengths of electromagnetic radiation at EEG frequencies.

Thus, neither the chemical diffusion, which is much too slow, nor the electric field of the extracellular dendritic current nor the magnetic fields inside the dendritic shafts, which are

much too weak, are the agency of the collective neuronal activity. Lashley's dilemma remains, thus, still to be explained.

The dissipative quantum model of the brain, which we compare with laboratory observations in this paper, has been proposed [28, 29] as an alternative approach to account for the observed dynamical formation of spatially extended domains of neuronal synchronized oscillations and of their rapid sequencing. The dissipative model explains indeed two main features of the EEG data [7]: the textured patterns of AM in distinct frequency bands correlated with categories of conditioned stimuli, i.e. *coexistence* of physically distinct AM patterns and the remarkably rapid onset of AM patterns into (irreversible) sequences that resemble cinematographic frames. Each spatial AM pattern is described to be consequent to spontaneous breakdown of symmetry (SBS) triggered by external stimulus and is associated with one of the emerging unitarily inequivalent ground states. Their sequencing is associated with the non-unitary time evolution implied by dissipation, as discussed below. It has to be remarked that the neuron and the glia cells and other physiological units are *not* quantum objects in the many-body model of the brain. This distinguishes the dissipative quantum model from all other quantum approaches to brain, mind and behavior. Moreover, the dissipative model describes the brain, not mental states. Also in this respect this model differs from those approaches where brain and mind are treated as if they were *a priori* identical.

In sections 2 and 3 we briefly summarize the main features of the original many-body model and its extension to dissipative dynamics, respectively. In section 4 we comment on the laboratory observations and their agreement with the dissipative model. We closely follow [7] in our presentation. Free energy, the arrow of time and classicality are discussed in sections 5 and 6, respectively. Conclusions are presented in section 7. For the reader's convenience and for completeness, details of the SBS mechanism in quantum field theory (QFT) and of the observational techniques are presented in appendices A and B, respectively.

## 2. The original many-body model

The dissipative quantum model [28], on which we focus our attention in this paper, extends the original quantum model of the brain to the dissipative dynamics intrinsic to the brain functional activity. The quantum model of the brain, here summarized briefly, was proposed in 1967 by Ricciardi and Umezawa [30] and further developed by Stuart, Takahashi and Umezawa [31], see also [32]. It was formulated in order to provide a solution to Lashley's dilemma. The model is primarily aimed at the description of memory storing and recalling. Umezawa explains the motivation for using the QFT formalism of many-body physics [33]: 'In any material in condensed matter physics any particular information is carried by certain ordered patterns maintained by certain long range correlations mediated by massless quanta. It looked to me that this is the only way to memorize some information; memory is a printed pattern of order supported by long range correlations . . .'

The main ingredient of the model is thus the mechanism of SBS by which long range correlations (the Nambu–Goldstone, briefly NG, boson modes) are dynamically generated (see appendix A). Water constitutes more than 80% to brain mass, and in the many-body model it is, therefore, expected to be a major facilitator or constraint on brain dynamics. The symmetry which gets broken is the rotational symmetry of the electric dipole vibrational field of the water molecules and of other biomolecules present in the brain structures [28, 34, 35]. The quantum variables are identified with those of the electric dipole vibrational field and with the associated NG modes, named the dipole wave quanta (DWQ). These are dynamically created and are not derived from Coulomb interaction.

If the cortex is at or near a singularity (see section 3), the external input or stimulus acts on the brain as a trigger for the breakdown of the dipole rotational symmetry. As a consequence long range correlation is established by the coherent condensation of DWQ bosons. SBS guarantees the change of scale, from the microscopic dynamics to the macroscopic order parameter field. The density value of the condensation of DWQ in the ground state (also called vacuum state) acts as a *label* classifying the state and thus the memory thereby created. The stored memory is not a representation of the stimulus, nor is it a collection of stimulus features. Indeed, a specific feature of the SBS mechanism in QFT is that the ordered pattern generated is controlled by the inner dynamics of the system, not by the external field (stimulus) whose only effect is the breakdown of the symmetry. This aspect of the model perfectly agrees with laboratory observations (see sections 3 and 4).

The recall of the recorded information occurs under the input of a stimulus capable of exciting DWQ out of the corresponding ground state. In the model, such a stimulus is called ‘similar’ to the one responsible for the memory recording [31]. Similarity is not an intrinsic property of the stimuli. Rather, it refers to their effects on the brain, namely inducing the formation or excitation of ‘similar’ ordered pattern(s).

One shortcoming of the many-body model in its original form is that any subsequent stimulus would cancel the previously recorded memory by renewing the SBS process and the consequent DWQ condensation, thus printing the new memory over the previous one (‘memory capacity problem’). Moreover, the model fails in explaining the observed coexistence of AM patterns and their irreversible time evolution. These problems are solved by endorsing the original many-body model with dissipative dynamics [28, 29], accounting for the fact that the brain is an open system in permanent interaction with its environment.

### 3. The dissipative many-body model

#### 3.1. Coherent states

The details of the coupling of the brain with the environment are very intricate and variable, and thus they are difficult to be characterized and measured. The external stimulus on the brain *selects* one vacuum state among infinitely many of them, unitarily inequivalent with each other (see appendix A). The selection of the vacuum is what happens in the process of SBS. The selected vacuum carries the *signature* (memory) of the reciprocal brain–environment influence at a given time under given boundary conditions. A change in the brain–environment interaction changes the choice of the vacuum: the brain evolution through the vacuum states thus reflects the evolution of the coupling of the brain with the surrounding world. The condensate of DWQ in the vacuum is assumed to be the quantum substrate of the observed AM patterns. In agreement with observations, the dissipative dynamics allows (quasi-)non-interfering degenerate vacua with different condensates. This corresponds to different AM patterns and (phase) transitions among them (AM pattern sequencing). These features could not be described in the framework of the original many-body model. By exploiting the existence of infinitely many inequivalent modes in QFT, the dissipative model allows a huge memory capacity. This can be seen as follows.

In QFT the canonical quantization of a dissipative system requires that the environment in which the system is embedded must also be included in the formalism. This is achieved by describing the environment as the time-reversed image of the system, and this is realized by doubling the system’s degrees of freedom [36]. In the dissipative quantum model, the brain dynamics is indeed described in terms of an infinite collection of damped harmonic oscillators  $a_\kappa$  (a simple prototype of a dissipative system) representing the boson DWQ modes [28] and by

the  $\tilde{a}_\kappa$  modes which are the time-reversed mirror images of the  $a_\kappa$  modes. The doubled modes  $\tilde{a}_\kappa$  represent the environment. The role of the  $\tilde{a}_\kappa$  system is to restore energy conservation by balancing the (in-/out-)energy fluxes. The label  $\kappa$  generically denotes degrees of freedom such as, e.g., spatial momentum, etc [28, 36, 37].

The  $a_\kappa$  and  $\tilde{a}_\kappa$  modes are massless NG modes. The system Hamiltonian is invariant under the dipole rotations (described by the  $SU(2)$  group). The breakdown of this rotational symmetry is induced by the external stimulus and this leads to the dynamical generation of DWQ  $a_\kappa$ . Their condensation in the ground state is then constrained by inclusion of the mirror modes  $\tilde{a}_\kappa$  in order to account for the system dissipation. The system ground state is indeed not invariant under (continuous) time translation symmetry. As a result, we have energy non-conservation and irreversible time evolution for the  $a_\kappa$  system. One can show [36, 37] that the external stimulus formally represents the coupling strength between the  $a_\kappa$  and the  $\tilde{a}_\kappa$  modes.

Although the living brain operates far from equilibrium, it evolves in time through a sequence of states where the energy fluxes and heat exchanges at the system–environment interface are balanced:  $E_{\text{sys}} - E_{\text{env}} \equiv E_0 = 0$ . This energy balance is manifested in the regulation of mammalian brain temperature. The balanced non-equilibrium system state, denoted by  $|0\rangle_{\mathcal{N}}$ , is thus the system vacuum or ground state. At some arbitrary initial time  $t_0 = 0$ , the Hamiltonian prescribes [28] that  $E_0 = \sum_\kappa \hbar \Omega_\kappa (\mathcal{N}_{a_\kappa} - \mathcal{N}_{\tilde{a}_\kappa}) = 0$ , where  $\Omega_\kappa$  is the common frequency of the  $a_\kappa$  and  $\tilde{a}_\kappa$  modes. This implies that the ‘memory state’  $|0\rangle_{\mathcal{N}}$  is a condensate of an *equal number* of modes  $a_\kappa$  and mirror modes  $\tilde{a}_\kappa$  for any  $\kappa$ :  $\mathcal{N}_{a_\kappa} - \mathcal{N}_{\tilde{a}_\kappa} = 0$ <sup>3</sup>. We have  ${}_{\mathcal{N}}\langle 0|0\rangle_{\mathcal{N}} = 1 \forall \mathcal{N}$ , where  $\mathcal{N}$  denotes the set of integers defining the ‘initial value’ of the condensate,  $\mathcal{N} \equiv \{\mathcal{N}_{a_\kappa} = \mathcal{N}_{\tilde{a}_\kappa}, \forall \kappa, \text{ at } t_0 = 0\}$ , as the *order parameter* associated with the information recorded at time  $t_0 = 0$ .

Clearly, balancing  $E_0$  to be zero does not fix the value of either  $E_{a_\kappa}$  or  $E_{\tilde{a}_\kappa}$  for any  $\kappa$ . It only fixes, for any  $\kappa$ , their difference. Therefore, at  $t_0$  we may have infinitely many perceptual states, each of which is in one-to-one correspondence to a given set  $\mathcal{N}$ . The dynamics ensures that the number  $(\mathcal{N}_{a_\kappa} - \mathcal{N}_{\tilde{a}_\kappa})$  is a constant of motion for any  $\kappa$  (see [28]). The average number  $\mathcal{N}_{a_\kappa}$  is given by

$$\mathcal{N}_{a_\kappa} = {}_{\mathcal{N}}\langle 0|a_\kappa^\dagger a_\kappa|0\rangle_{\mathcal{N}} = \sinh^2 \theta_\kappa, \tag{1}$$

where  $\theta_\kappa$  is a transformation parameter. The  $\theta$ -set,  $\theta \equiv \{\theta_\kappa, \forall \kappa, \text{ at } t_0 = 0\}$ , is related to the  $\mathcal{N}$ -set,  $\mathcal{N} \equiv \{\mathcal{N}_{a_\kappa} = \mathcal{N}_{\tilde{a}_\kappa}, \forall \kappa, \text{ at } t_0 = 0\}$ , by equation (1). We also use the notation  $\mathcal{N}_{a_\kappa}(\theta) \equiv \mathcal{N}_{a_\kappa}$  and  $|0(\theta)\rangle \equiv |0\rangle_{\mathcal{N}}$ . The  $\theta$ -set is conditioned by the requirement that  $a_\kappa$  and  $\tilde{a}_\kappa$  modes satisfy the Bose–Einstein distribution:

$$\mathcal{N}_{a_\kappa}(\theta) = \sinh^2 \theta_\kappa = \frac{1}{e^{\beta E_\kappa} - 1}, \tag{2}$$

where  $\beta \equiv \frac{1}{k_B T}$  is the inverse temperature at time  $t_0 = 0$  ( $k_B$  is Boltzmann’s constant).  $|0\rangle_{\mathcal{N}}$  is thus recognized to be a finite temperature state and it can be shown to be a squeezed coherent state [28, 38–40].

The spaces  $\{|0\rangle_{\mathcal{N}}\}$  and  $\{|0\rangle_{\mathcal{N}'}\}$  are unitarily inequivalent with each other for different labels  $\mathcal{N} \neq \mathcal{N}'$  in the infinite volume limit. This is expressed by the relation:

$${}_{\mathcal{N}}\langle 0|0\rangle_{\mathcal{N}'} \xrightarrow{V \rightarrow \infty} 0 \quad \forall \mathcal{N}, \mathcal{N}', \quad \mathcal{N} \neq \mathcal{N}'. \tag{3}$$

We have, therefore, infinitely many unitarily inequivalent spaces of states  $\{|0\rangle_{\mathcal{N}}\}$ . The set of all these spaces constitutes the whole space of states. A huge number of sequentially recorded

<sup>3</sup> Let  $\{|\mathcal{N}_{a_\kappa}, \mathcal{N}_{\tilde{a}_\kappa}\rangle\}$  be the set of simultaneous eigenvectors of  $\hat{N}_{a_\kappa} \equiv a_\kappa^\dagger a_\kappa$  and  $\hat{N}_{\tilde{a}_\kappa} \equiv \tilde{a}_\kappa^\dagger \tilde{a}_\kappa$ , with  $\mathcal{N}_{a_\kappa}$  and  $\mathcal{N}_{\tilde{a}_\kappa}$  being non-negative integers. Then  $|0\rangle_0 \equiv |\mathcal{N}_{a_\kappa} = 0, \mathcal{N}_{\tilde{a}_\kappa} = 0\rangle$  denotes the state annihilated by  $a_\kappa$  and by  $\tilde{a}_\kappa$ :  $a_\kappa|0\rangle_0 = 0 = \tilde{a}_\kappa|0\rangle_0$  for any  $\kappa$ .

memories may thus *coexist* without destructive interference since infinitely many vacua  $|0\rangle_{\mathcal{N}}$  are independently accessible. In contrast to the non-dissipative model, recording the memory  $\mathcal{N}'$  does not necessarily produce destruction of a previously printed memory  $\mathcal{N} \neq \mathcal{N}'$ ; this is the meaning of the non-overlapping modes in the infinite volume limit expressed by equation (3). Through the doubled degrees of freedom  $\tilde{a}_k$ , dissipation allows the possibility of a huge memory capacity by introducing the  $\mathcal{N}$ -labelled ‘replicas’ of the ground state. The dissipative model, thus, predicts the existence of textures of AM patterns (cf section 4),

These patterns are represented by order parameters that are stable against quantum fluctuations. This is a manifestation of the *coherence* of the DWQ boson condensation. In this sense, the order parameter is a macroscopic observable and the state  $|0\rangle_{\mathcal{N}}$  provides an example of the macroscopic quantum state. The change of scale (from microscopic to macroscopic) is dynamically achieved through the SBS leading to boson condensation.

### 3.2. Phase transitions

The brain (ground) state may be represented as the collection (or the superposition) of the full set of states  $|0\rangle_{\mathcal{N}}$ , for all  $\mathcal{N}$ . In the memory space or the *brain state space*, each representation  $\{|0\rangle_{\mathcal{N}}\}$  denotes a physical phase of the system and may be conceived as a ‘point’ identified by a specific  $\mathcal{N}$ -set (or  $\theta$ -set). In the infinite volume limit, points corresponding to different  $\mathcal{N}$  (or  $\theta$ ) sets are distinct points (do not overlap, cf equation (3)). The brain in relation to the environment may occupy any of the ground states, depending on how the  $E_0 = 0$  balance is approached. Or, it may be in any state that is a collection or superposition of these brain-environment equilibrium ground states. Under the influence of one or more stimuli (acting as control parameters), the system may shift from ground state to ground state in this collection (from phase to phase), namely it may undergo an extremely rich sequence of phase transitions, leading to the actualization of a sequence of dissipative structures formed by AM patterns (see section 4).

Let  $|0(t)\rangle_{\mathcal{N}}$  denote the state  $|0\rangle_{\mathcal{N}}$  at time  $t$  specified by the initial value  $\mathcal{N}$ , at  $t_0 = 0$ . We have  ${}_{\mathcal{N}}\langle 0(t)|0(t)\rangle_{\mathcal{N}} = 1, \forall t$ . We can show that

$$\lim_{t \rightarrow \infty} {}_{\mathcal{N}}\langle 0(t)|0\rangle_{\mathcal{N}} \propto \lim_{t \rightarrow \infty} \exp\left(-t \sum_{\kappa} \Gamma_{\kappa}\right) = 0, \quad (4)$$

provided  $\sum_{\kappa} \Gamma_{\kappa} > 0$ . In the infinite volume limit we have (for  $\int d^3\kappa \Gamma_{\kappa}$  finite and positive)

$${}_{\mathcal{N}}\langle 0(t)|0(t')\rangle_{\mathcal{N}} \xrightarrow{V \rightarrow \infty} 0 \quad \forall t, t', \quad t \neq t'. \quad (5)$$

The time evolution of the state  $|0(t)\rangle_{\mathcal{N}}$  is thus represented as the trajectory starting with ‘initial condition’ specified by the  $\mathcal{N}$ -set in the space  $\{|0(t)\rangle_{\mathcal{N}}\}$ . In a pictorial way we could say that the state  $|0(t)\rangle_{\mathcal{N}}$  provides the ‘instantaneous picture’ of the system at each instant of time  $t$  or the ‘photograph’ at  $t$  in a cinematographic sequence.

Time-dependence of the DWQ frequency implies that higher momentum  $\kappa$ -components of the  $\mathcal{N}$ -set possess longer life-times. Momentum is proportional to the inverse distance over which the mode propagates; thus modes with a shorter range of propagation (more ‘localized’ modes) survive longer. In contrast, modes with a longer range of propagation decay sooner.

As a result, condensation domains of different finite sizes with different degrees of stability are predicted by the model [37]. They are described by the condensation function  $f(x)$  which acts as a ‘form factor’ specific for the considered domain [38, 41, 42].  $f(x)$  has to carry some topological singularity in order for the condensation process to be physically detectable. A regular function  $f(x)$  would produce a condensation which could be easily ‘washed’ out (‘gauged’ away by a convenient gauge transformation). In a similar way, the

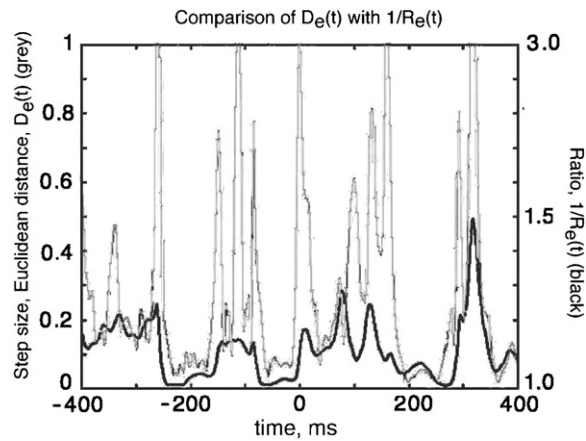


**Figure 1.** The sharp spikes (gray,  $D_e(t)$ ) show the rate of change in spatial AM pattern. The lower curve (black, the inverse of  $R_e(t)$ , a measure of synchrony) shows that re-synchronization precedes the emergence of spatial order and also the increase in power in each frame (see also figure B1). (This figure is in colour only in the electronic version)

phase transition from one space to another (inequivalent) space can only be induced by a singular condensation function  $f(x)$ . This explains why topologically non trivial extended objects, such as vortices, appear in phase transitions [38, 41, 42]. Phase transitions driven by boson condensation are always associated with some singularity (indeterminacy) in the field phase at the phase transition point [43]. This model feature accounts for a crucial mechanism observed in laboratory experiments: the event that initiates a perceptual phase transition is an abrupt decrease in the analytic power of the background activity to near zero.

#### 4. Observation in cortical dynamics

The high spatial resolution required to measure AM pattern textures in brain activity is achieved by using high-density electrode arrays, fixed on the scalp or the epidural surface of cortical areas and fast Fourier transform (FFT) [8, 44]. The set of  $n$  amplitudes squared from an array of  $n$  electrodes (typically 64) defines a feature vector,  $\mathbf{A}^2(t)$ , of the spatial pattern of power at time  $t$ . The vector specifies a point on a dynamic trajectory in *brain state space*, conceived as the collection of all possible (essentially infinitely many) brain states. The measurement of  $n$  EEG signals defines a finite  $n$ -dimensional subspace, so the point specified by  $\mathbf{A}^2(t)$  is unique for a spatial AM pattern of an aperiodic carrier wave. Similar AM patterns form a cluster in  $n$ -space, and multiple patterns form either multiple clusters or trajectories with large Euclidean distances between the digitizing steps in  $n$ -space. A cluster with a verified behavioral correlate denotes an *ordered AM pattern*: when the trajectory of a sequence of points enters into a cluster, that location in state space signifies increased order from the perspective of an intentional state of the brain, owing to the correlation with a conditioned stimulus (for further details see appendix B).

The inverse of the absolute value of the step size between successive values of  $D_e(t) = |\mathbf{A}^2(t) - \mathbf{A}^2(t-1)|$  provides a scalar index of the order parameter. Indeed, small steps in Euclidean distances,  $D_e(t)$  (higher spikes in figure 1) indicate pattern amplitude stability. Pattern phase stability can be characterized by calculating the ratio,  $R_e(t)$ , of the temporal

standard deviation of the mean filtered EEG to the mean temporal standard deviation of the  $n$  EEGs [10, 11] (lower curve in figure 1).  $R_e(t) = 1$  when the oscillations are completely synchronized. When  $n$  EEGs are totally desynchronized,  $R_e(t)$  approaches one over the square root of the number of digitizing steps in the moving time window. It was experimentally found that  $R_e(t)$  rises rapidly within a few ms after a phase discontinuity and several ms before the onset of a marked increase in mean analytic amplitude,  $\underline{A}(t)$ .

The succession of the high and low values of  $R_e(t)$  reveals the episodic emergence and dissolution of synchrony; since cortical transmission of spatial patterns is most energy efficient when the dendritic currents are most synchronized,  $R_e(t)$  can be adopted as an index of cortical *efficiency* [46]. Re-synchronized oscillations in the beta range near zero lag commonly recur at rates in the theta range. They cover substantial portions of the left cerebral hemisphere [9], in some instances appearing to exceed the length of the recording array (19 cm) on the scalp above the human brain.

Assuming that the phenomenological order parameter  $\mathbf{A}^2(t)$  corresponds to the order parameter  $\mathcal{N}$  introduced in the dissipative model, the trajectories described by the time-dependent vector  $\mathbf{A}^2(t)$  in the brain state space have their quantum image in the time evolution in the spaces  $\{|0\rangle_{\mathcal{N}}\}$ .

Considering the common frequency  $\Omega_{\kappa}(t)$  for the  $a_{\kappa}$  and  $\tilde{a}_{\kappa}$  modes (cf equation (8) in [37]) in the dissipative model, the duration, size and power of AM patterns are predicted to be decreasing functions of the carrier wave number  $\kappa$ . This is confirmed by the observations. Carrier waves in the gamma range (30–80 Hz) show durations seldom exceeding 100 ms, diameters seldom exceeding 15 mm; and low power in a  $1/f^a$  power law as a function of frequency. Carrier frequencies in the beta range (12–30 Hz) show durations often exceeding 100 ms; estimated diameters are large enough to include multiple primary sensory areas and the limbic system; and they have greater power.

The reduction in the amplitude of the spontaneous background activity induces a brief state of instability, depicted as a null spike [45], in which the significant pass band of the ECoG is near to zero and its phase is undefined, as indeed predicted by the dissipative model. The cortex can be driven across the phase transition process to a new AM pattern by the stimulus arriving at or just before this state. When considering the normalized amplitude defined as the AM pattern divided by the mean amplitude, which is input dependent, one observes that, again in agreement with prediction of the dissipative model, such a normalized response amplitude depends not on the input amplitude, but on the intrinsic state of the cortex, specifically the degree of reduction in the power and order of the background brown noise. The null spike in the band pass filtered brown noise activity is conceived as a *shutter* that blanks the intrinsic background. At very low analytic amplitude when the analytic phase is undefined, the system, under the incoming weak sensory input, may reset the background activity in a new AM frame, if any, formed by reorganizing the existing activity, not by the driving of the cortical activity by input (except for the small energy provided by the stimulus that is required to force the phase transition (and select an attractor, see below)). The decrease (*shutter*) repeats aperiodically in the theta or alpha range, independently of the repetitive sampling of the environment by limbic input and allows opportunities for phase transitions.

In conclusion, the reduction in activity constitutes a singularity in the dynamics at which the phase is undefined, in agreement with the dissipative model requiring the singularity of the boson condensation function. The power is not provided by the input, exactly as the dissipative model predicts, but by the pyramidal cells, which explains the lack of invariance of AM patterns with invariant stimuli [45].

Finally, we note that another possible way to break the symmetry in QFT is to modify the dynamical equations by adding one or more terms that are explicitly not consistent with the

symmetry transformations (i.e., are not symmetric terms). This is called *explicit* breakdown of symmetry. The system is forced by the external action into a specific non-symmetric state that is determined by the imposed breaking term. The explicit breakdown fits well with *event-related potentials* (ERP) observed as the response of the cortex to perturbations, such as an electric shock, sensory click, flash, or touch. By resorting to stimulus-locked averaging across multiple presentations in order to remove or attenuate the background activity, the location, intensity and detailed configuration of the ERP are predominantly determined by the stimulus; so ERP signals can be used as evidence for processing by the cortex of exogenous information. In contrast, in SBS pattern configurations are determined from information that is endogenous from the memory store.

### 5. The thermal connection: free energy and the arrow of time

In section 3 we have seen that the brain states  $|0\rangle_{\mathcal{N}}$  are finite temperature states. This shows the intrinsically thermal nature of brain dynamics which we analyze further in the present section.

In the dissipative model, the free energy functional for the  $a_{\kappa}$  modes is given by [28]

$$\mathcal{F}_a \equiv {}_{\mathcal{N}}\langle 0(t) | \left( H_a - \frac{1}{\beta} S_a \right) | 0(t) \rangle_{\mathcal{N}}, \quad (6)$$

with time-dependent inverse temperature  $\beta(t) = \frac{1}{k_B T(t)}$ .  $S_a$  is the entropy operator given by

$$S_a \equiv - \sum_{\kappa} \{ a_{\kappa}^{\dagger} a_{\kappa} \ln \sinh^2 \Theta_{\kappa} - a_{\kappa} a_{\kappa}^{\dagger} \ln \cosh^2 \Theta_{\kappa} \}, \quad (7)$$

where  $\Theta_{\kappa} \equiv \Gamma_{\kappa} t - \theta_{\kappa}$ . Here  $\Gamma_{\kappa}$  is the damping constant and  $\theta_{\kappa}$  is the transformation parameter introduced in equation (1).  $S_{\tilde{a}}$  is obtained by replacing  $a_{\kappa}$  and  $a_{\kappa}^{\dagger}$  with  $\tilde{a}_{\kappa}$  and  $\tilde{a}_{\kappa}^{\dagger}$ , respectively, in (7).  $H_a$  denotes the Hamiltonian at  $t = t_0$  relative to the  $a_{\kappa}$ -modes only,  $H_a = \sum_k E_k a_k^{\dagger} a_k$ , with  $E_k \equiv \hbar \Omega_k(t_0)$ . For the complete system  $a - \tilde{a}$ , the difference ( $S_a - S_{\tilde{a}}$ ) is constant in time:  $[S_a - S_{\tilde{a}}, \mathcal{H}'] = 0$ . The stationarity condition to be satisfied at each time  $t$  by the state  $|0(t)\rangle_{\mathcal{N}}$  is  $\frac{\partial \mathcal{F}_a}{\partial \Theta_k} = 0, \forall k$ , which, for  $\beta(t)$  slowly varying in time, i.e.  $\frac{\partial \beta}{\partial t} = -\frac{1}{k_B T^2} \frac{\partial T}{\partial t} \approx 0$ , gives the Bose–Einstein distribution

$$\mathcal{N}_{a_k}(\theta, t) = \frac{1}{e^{\beta(t) E_k} - 1}. \quad (8)$$

The changes in the energy  $E_a \equiv \sum_k E_k \mathcal{N}_{a_k}$  and in the entropy  $S_a(t) = \langle 0(t) | S_a | 0(t) \rangle_{\mathcal{N}}$  are given by

$$dE_a = \sum_k E_k \dot{\mathcal{N}}_{a_k} dt = \frac{1}{\beta} dS_a. \quad (9)$$

Provided that changes in inverse temperature are slow, the minimization of the free energy thus holds at any  $t$ :

$$d\mathcal{F}_a = dE_a - \frac{1}{\beta} dS_a = 0. \quad (10)$$

The time evolution of the state  $|0(t)\rangle_{\mathcal{N}}$  at finite volume  $V$  can be shown [28, 36] to be controlled by the entropy variations, which reflects the irreversibility of time-evolution (breakdown of time-reversal symmetry) characteristic of dissipative systems. This corresponds to the choice of a privileged direction in time-evolution called *arrow of time*.

Equation (9) shows that the change in time of the condensate, i.e. of the order parameter, turns into heat dissipation  $dQ = \frac{1}{\beta} dS_a$ . Therefore, the ratio of the rate of free energy

dissipation to the rate of change of the order parameter is a good measure of the ordering stability. In terms of laboratory observations, the rate of change of the order parameter is specified by the Euclidean distance  $D_e(t)$  between successive points in the  $n$ -space.  $D_e(t)$  takes large steps between clusters, decreases to a low value when the trajectory enters a cluster and remains low for tens of ms within a frame (figure 1). Therefore  $D_e(t)$  serves as a measure of the spatial AM pattern stability.

It was found [6, 12] that the best predictor for the onset of ordered AM patterns is the *pragmatic information* index  $H_e(t)$ , so named after Atmanspacher and Scheingraber [47], given by the ratio of the rate of free energy dissipation  $\underline{A}^2(t)$  to the rate of change of the order parameter represented by  $D_e(t)$  (because  $D_e(t)$  falls and  $\underline{A}^2(t)$  rises with wave packet evolution):

$$H_e(t) = \frac{\underline{A}^2(t)}{D_e(t)}.$$

Measurements showed that typically the rate of change in the instantaneous frequency  $\omega(t)$  was low in frames that coincided with low  $D_e(t)$  indicating stabilization of frequency as well as AM pattern. Between frames  $\omega(t)$  often increased several times or decreased even below zero in interframe breaks that repeat at rates in the theta or alpha range of the EEG [9] (*phase slip* [48]).

We observe that the mirror  $\tilde{a}_\kappa$  modes account [50, 49] for Brownian quantum noise due to the fluctuating random force in the system–environment coupling. Such a noise is responsible for the fact that the state  $|0\rangle_{\mathcal{N}}$  is an entangled state [7], the entropy operator providing a measure of the entanglement ( $a_\kappa$  and  $\tilde{a}_\kappa$  modes are entangled modes). In other words, the brain processes are inextricably dependent on the quantum noise in the fluctuating random force in the brain–environment coupling. There is a permanent brain–environment entanglement. This feature seems to model the observed continual perturbations involving all areas of neocortex by other parts of the brain, including inputs from the sensory receptors that are relayed mainly through the thalamus and the catastrophic disruptions of brain function that result from prolonged sensory deprivation. These continuous perturbations give rise to myriads of local phase transitions, which are quenched as rapidly as they are formed, thereby maintaining the entire cortex in a robust state of conditional stability (metastability [51–53]). An interesting question is whether such a regime might conform to self-organized criticality [6, 8, 54–56] (the mean firing rate of neurons, homeostatically maintained by mutual excitation everywhere by thresholds and refractory periods, would play the role of the critical variable corresponding to angle in self-organized criticality [11]). It is indeed interesting that, in a model [57] based on self-organized criticality combined with synaptic plasticity in a neural network, the average power spectrum computed as a function of frequency exhibits a power law behavior with the same exponent as found in medical EEG power spectra [44, 58].

## 6. Classicality and attractor landscapes: the classical blanket

One of the merits of the dissipative many-body model is the possibility [28, 29, 37, 49] of deriving from the microscopic dynamics the classicality of the trajectories representing the time evolution of the state  $|0(t)\rangle_{\mathcal{N}}$  in the brain state space. These trajectories are found to be deterministic chaotic trajectories [49, 59]. This is a particularly welcome feature of the model since observed changes in the order parameter become susceptible to be described in terms of trajectories on attractor landscapes. One can show these trajectories are *classical* and that

- (i) they are bounded and do not intersect themselves (trajectories are not periodic);
- (ii) there are no intersections between trajectories specified by different initial conditions;

(iii) trajectories of different initial conditions diverge.

Although property (ii) implies that no *confusion* or interference arises among different memories, even as time evolves, states with different  $\mathcal{N}$  labels may have non-zero overlap (non-vanishing inner products) in realistic situations of finite volume. This means that some *association* of memories becomes possible: at a ‘crossing’ point between two, or more than two, trajectories, one can ‘switch’ from one of them to another one. This reminds us of the ‘mental switch’ occurring during particular perceptual and motor tasks [51, 60] as well as during free associations in memory tasks [61].

One can derive [49] from property (iii) that the difference between  $\kappa$ -components of the sets  $\mathcal{N}$  and  $\mathcal{N}'$  may become zero at a given time  $t_\kappa$ . However, the difference between the sets  $\mathcal{N}$  and  $\mathcal{N}'$  does not necessarily become zero. The  $\mathcal{N}$ -sets are made up of a large number (infinite in the continuum limit) of  $\mathcal{N}_{a_\kappa}(\theta, t)$  components, and they are different even if a finite number (of zero measure) of their components are equal. In contrast, for very small  $\delta\theta_\kappa$ , suppose that  $\Delta t \equiv \tau_{\max} - \tau_{\min}$ , with  $\tau_{\min}$  and  $\tau_{\max}$  the minimum and the maximum, respectively, of  $t_\kappa$ , for all  $\kappa$ s, be ‘very small’. Then the  $\mathcal{N}$ -sets are ‘recognized’ to be ‘almost’ equal in such a  $\Delta t$ . Thus, we see how in the ‘recognition’ (or recall) process it is possible that ‘slightly different’  $\mathcal{N}_{a_\kappa}$ -patterns are ‘identified’ (recognized to be the ‘same pattern’ even if corresponding to slightly different inputs). Roughly,  $\Delta t$  provides a measure of the ‘recognition time’.

The deterministic chaotic motion described by (i)–(iii) takes place in the space of the parameters labelling the system ground state. It is low dimensional and noise-free. In a more realistic framework, the motion must be conceived as high-dimensional, noisy, engaged and time varying. Nevertheless, it is remarkable that, at the present stage of our research, the dissipative model predicts that the system trajectories through its physical phases may be chaotic [49] and itinerant through a chain of ‘attractor ruins’ [62], embedded in a set of attractor landscapes [63] accessed serially or merely approached in the coordinated dynamics of a metastable state [50, 52, 65, 53, 64]. The manifold on which the attractor landscapes sit covers as a *classical blanket* the quantum dynamics going on in each of the representations of the CCRs (the AM patterns recurring at rates in the theta range (3 – 8 Hz)).

We propose conditioned stimuli *select* a basin of attraction in the primary sensory cortex to which it converges (*abstraction* by deletion of nonessential information), often with very little information as in weak scents, faint clicks and weak flashes. The astonishingly low requirements for information in high-level perception have been amply demonstrated by recent accomplishments in sensory substitution [66, 67, 4]. There is an indefinite number of such basins forming a pliable and adaptive attractor landscape in each sensory cortical area. Each attractor can be selected by a stimulus that is an instance of the category (*generalization*) that the attractor implements by its AM pattern. The waking state consists of a collection of potential states, any one of which (but only one at a time) can be realized through a phase transition. The variety of these highly textured, latent AM patterns, their exceedingly large diameters in comparison to the small sizes of the component neurons and the extraordinarily rapid temporal sequence in the neocortical phase transitions by which they are selected, provide the principal justification for exploring the interpretation of nonlinear brain dynamics in terms of many-body theory and multiple ground states.

## 7. Concluding remarks

Our discussion in this paper leads us to conclude that the dissipative quantum model of brain predicts two main features observed in neurophysiological data: the coexistence of physically distinct AM patterns correlated with categories of conditioned stimuli and the remarkably rapid

onset of AM patterns into irreversible sequences that resemble cinematographic frames. Each spatial AM pattern is described to be consequent to the spontaneous breakdown of symmetry triggered by an external stimulus and is associated with one of the unitarily inequivalent ground states of QFT. Their sequencing is associated with the non-unitary time evolution implied by dissipation. There are many open questions which remain to be answered. For example, the analysis of the interaction between the boson condensate and the details of electrochemical neural activity, or the problems of extending the dissipative many-body model to account for higher cognitive functions of the brain need much further work.

One peculiar property of quantum field dynamics, which makes it so successful in the description of many-body systems with different phases, and which motivates us to apply it to brain dynamics, is that there are many stability ranges, each one characterizing a specific phase of the system with specific physical properties that differ from phase to phase (in the brain: from each observed AM pattern to the next). If the dynamical regime is characterized by a range of parameter values which does not allow SBS, the system does not perceptibly or meaningfully react (as in sleep to weak stimuli). When one or more control parameters, such as the strength of action at one class of synapses in the cortical pool under the influence of the weak external stimulus, or even by indeterminate drift, exceeds the range of stability where the system originally sits, a transition is induced to another stability parameter range. It differs from the previous one in that it now allows SBS and the appearance of order (as in arousal from deep sleep). Contrarywise, the loss of order as in shutting down under anesthesia or in deep sleep corresponds to symmetry recovery or restoration, the formlessness of background activity or in the extreme the loss of activity in the case of brain death.

The concept of the DWQ boson carrier discussed above enables an orderly and inclusive description of the phase transition that includes all levels of the microscopic, mesoscopic, and macroscopic organization of cerebral patterns. The hierarchical structure extending from atoms to the whole brain and outwardly into engagement of the subject with its environment in the action–perception cycle is the essential basis for the emergence and maintenance of meaning through successful interaction and its knowledge base within the brain. By repeated trial-and-error each brain constructs within itself an understanding of its surrounding, which constitutes its *knowledge* of its own world that we describe as its *Double* [29]. It is an *active* mirror, because the environment impacts onto the self independently as well as reactively. The notion of an order parameter denotes a categorical descriptor that exists only in the brain, so that its matching ‘double’ is a finite projection from the brain into the environment, as the basis for organizing the action of the body governed by the brain. An example is the grasping of an object by the hand, described by the phenomenologist Merleau-Ponty [68] as the achievement of ‘maximum grip’. Thus, we conceive the ‘double’ as the descriptor of the perception or experience of the object, as contrasted with the brain activity pattern that is matched by the ‘double’. Such a matching is formally described by the continual balancing of the energy fluxes at the brain–environment interface. It amounts to the continual updating of the *meanings* of the flow of information exchanged in the brain behavioral relation with the environment.

Perhaps, at the present status of our research, we might conclude that the dissipative quantum dynamics underlying textured AM patterns and sequential phase transitions observed in brain functioning could open the way to understand John von Neumann’s remark: ‘... the mathematical or logical language truly used by the central nervous system is characterized by less logical and arithmetical depth than what we are normally used to. ... We require exquisite numerical precision over many logical steps to achieve what brains accomplish in very few short steps’ (pp 80–81 of [69]).

## Acknowledgments

The authors thank Prof. Mariano A del Olmo and the organizers of the International Conference ‘Quantum Theory and Symmetries, QTS-5’, held in Valladolid, Spain, July 2007, for giving them the opportunity to present in that Conference the results reported in this paper. Partial financial support from MUR and INFN is also acknowledged.

## Appendix A. Spontaneous breakdown of symmetry in quantum field theory

Symmetry is said to be spontaneously broken when the Lagrangian of a system is invariant under a certain group of continuous symmetry, say  $G$ , and the vacuum or ground state of the system is not invariant under  $G$ , but under one of its subgroups, say  $G'$  [38, 70, 71]. The ground state then exhibits observable ordered patterns corresponding to the breakdown of  $G$  into  $G'$  [38, 71, 72]. The possibility of having different vacua with different symmetry properties is provided by the mathematical structure of QFT, where infinitely many representations of the canonical commutation relations (CCR) exist, which are unitarily inequivalent with respect to each other, i.e there is no unitary operator transforming one representation into another one [73], and thus they are physically inequivalent as well: they describe different physical phases of the system. By contrast, in quantum mechanics all representations are unitarily (and therefore physically) equivalent [38, 74, 75].

In SBS theories, the Goldstone theorem predicts the existence of massless bosons, called Nambu–Goldstone (NG) particles [76]. The spin-wave quanta, called magnons in ferromagnets, the elastic wave quanta, called phonons in crystals, the Cooper pair quanta in superconductors, etc [38, 71], are examples of NG particles. NG bosons condensed in the ground state of the system according to the Bose–Einstein condensation are the carriers of ordering information out of which ordered patterns (space ordering or time ordering as, e.g., ‘in phase’ oscillations) are generated. The condensation density of the NG boson quanta determines the macroscopic field which is called *order parameter*, e.g. the magnetization in ferromagnets. The order parameter is a classical macroscopic field in the sense that it is not affected by quantum fluctuations. Its value may be considered to be the *code* or *label* specifying the physical phase of the system.

In the absence of gauge fields, the NG quanta are observed as realistic physical quanta, and excitations of the vacuum extend over the whole system (*collective modes* or *long range correlations*). They may scatter with other particles of the system or with observational probes. If a gauge field is present, the NG bosons still control the condensation in the ordered domain, and the gauge field propagation is confined into regions where the order is absent (e.g. in the core of the vortex in superconductors, Anderson–Higgs–Kibble mechanism) [38, 71, 77, 78].

Through the generation of NG collective modes, SBS is responsible for the change from the microscopic to macroscopic scale [38, 71]: crystals, ferromagnets, superconductors, etc are *macroscopic quantum systems*. They are quantum systems not in the sense that they constitute of quantum components (like any physical system), but in the sense that their macroscopic properties, accounted for by the order parameter field, cannot be explained without recourse to the underlying quantum dynamics.

We finally comment on the Hermitian conjugation of the Hamiltonian in the real-time finite temperature formalism (thermo field dynamics (TFD)), where there are three free parameters,  $f, \alpha, s$ , in the notation of [38], corresponding to the three parameters of the  $SU(1, 1)$  group. The parameter  $s$  does not contribute to the propagator [38] and is usually set equal to zero since no physical meaning is attached to it.  $\alpha$  is related to the cyclic property of the trace operation  $\text{Tr}[\rho A] = \text{Tr}[\rho^{1-\alpha} A \rho^\alpha]$ . Physical observables are independent of  $\alpha$ . The choice  $\alpha = 1$  (or

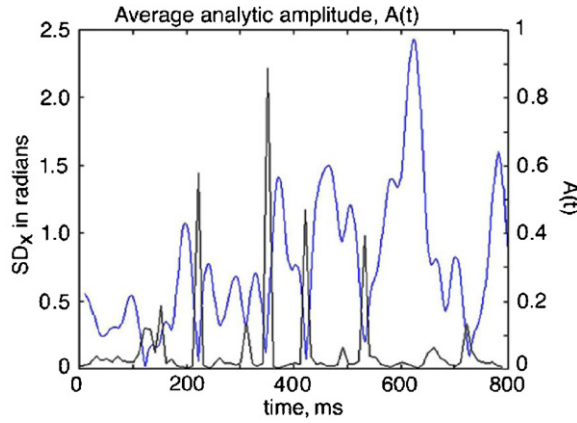


**Figure B1.** The analytic amplitude,  $A(t)$ , of the ECoG in the beta band fluctuates with time. The maxima are textured with AM spatial patterns. The minima are accompanied by spikes in the spatial standard deviation of the phase differences as a function of time,  $SDx(t)$ . Each spike reflects the indeterminacy of phase at the null spike in amplitude, where a phase transition is enabled.

$\alpha = 0$ ) turns out to be convenient in Feynman graph computations in non-equilibrium TFD [40, 38]. The choice  $\alpha = \frac{1}{2}$  preserves the usual definition of Hermitian conjugation. Other choices give the so-called non-Hermitian representations of TFD. Since the physical content of the model is not affected, we use  $\alpha = \frac{1}{2}$ , as far as we are not involved in computations of Feynman graphs. The parameter  $f$  is the only physically relevant parameter. It is related to the canonical Bose distribution (2), in which case it is  $f = e^{-\beta E}$ , and thus it determines the  $\mathcal{N}_{A_k}$ s.

## Appendix B. Neurophysiological observations

The tight sequencing of AM patterns requires high temporal resolution. Hilbert transform is then applied to EEG signals after band pass filtering [8, 10, 11]. Unlike the Fourier transform that decomposes an extended time series into fixed frequency components, the Hilbert transform decomposes an EEG signal into the analytic amplitude  $A(t)$ , the analytic phase  $P(t)$  and the instantaneous frequency,  $\omega(t)$ , at each digitizing time step on each channel.

The analytic phase difference  $\Delta P_j(t) = P_j(t) - P_j(t - 1)$  at each electrode and at each digitizing step divided by the digitizing time increment specifies the instantaneous frequency:  $\omega_j(t) = \frac{\Delta P_j(t)}{\Delta t}$ . It has been shown in [10] that the rate of increase in phase (the mean instantaneous frequency = 0.4 rad/2 ms = 31 Hz) is relatively constant in epochs that last ~60–100 ms and that recur at intervals in the theta and alpha ranges. These plateaus in nearly constant phase increase are bracketed by phase discontinuities synchronized across the array [10]. This spatially correlated ‘phase slip’ demarcates *phase transitions* in the cortical dynamics. The brackets are detected and displayed as spikes (see figure B1) by calculating the spatial standard deviation of the phase differences,  $SDx(t)$ , across the array as a time series for the 64 signals.  $SDx(t)$  is thus a useful index of the temporal stability. The spikes bracket the stabilized epochs and define the beginning and end of wave packets; the plateaus demarcate epochs of near stationarity.

Calculation of  $SD_X(t)$ , and the mean analytic amplitude  $\underline{A}(t)$  across  $n$  channels at each time point confirmed [10, 11, 79] that peaks in  $\underline{A}(t)$  accompany plateaus in  $SD_X(t)$  (figure B1). Peak amplitudes enable optimal measurement of spatial patterns of AM of beta or gamma carrier frequency. Each pattern is expressed by an  $n \times 1$  feature vector in the square of amplitude,  $A_j^2(t)$ . The mean power,  $\underline{A}^2(t)$ , serves as a scalar label for each AM pattern.

These broad AM patterns are the neural correlates to display the rapid re-organization of brain activity that we believe underlies both cognitive function and sequences of complex intentional behaviors. Owing to the potential differences that dendritic currents maintain as they flow across the relatively fixed extracellular impedance of the neuropil, the values of  $A_j^2(t)$  provide a measure of the rates of free energy dissipation required by the neurons generating the ECoG. Our index of those energy levels may be optimally correlated with patterns of increased blood flow that indirectly manifest the metabolic energy utilization by parts of the brains, which are detected with fMRI, PET and SPECT [80].

At first view the AM patterns appear to be ‘cortical representations’ of conditioned stimuli (CS). However, the patterns that are elicited by an invariant CS hold only within each training session and then only if there are no changes in the schedule of reinforcement or addition of a new CS in serial conditioning. Measurements of AM patterns within sessions show pattern variation within each category despite CS invariance. Between sessions with no new CS added the averages of the patterns tend to drift. When the subjects are trained to respond to a new CS, all of the patterns change, including the pattern for the background. The amount of change with new learning is two to four times the average change with drift across multiple sessions [81–83]. A collection of AM patterns that we established by training persisted with drift through multiple sessions until we introduced the next contextual change.

Every AM pattern is accompanied by a conic phase pattern that retains the history of its site of nucleation and spread. Phase cones were also found between ordered frames and overlapping with them at near and far frequencies. In a distributed medium such as the neuropil, the generation of the cortical standing wave resulting from a phase transition forming a wave packet begins at a site of nucleation and spreads radially at a velocity determined by the propagation velocities of axons extending parallel to the surface. This gives a conic phase gradient and the illusion of a travelling wave by the delay in initialization embodied in the phase cone. This is measured by fitting a cone to a phase surface given by the analytic phase,  $P_j(t)$ ,  $j = 1, \dots, 64$ . The phase transitions appear to be induced by input to the cortex serving as a control parameter; however, the latency varies randomly with respect to known times of input onset.

On successive trials with the same CS, the location of the apex varies randomly within the primary receiving area for the CS modality, and its sign (maximal lead as in an explosion or maximal lag as in an implosion) likewise varies randomly from each phase transition to the next. These random variations give further evidence for SBS [43].

## References

- [1] Lashley K 1948 *The Mechanism of Vision, XVIII, Effects of Destroying the Visual ‘Associative Areas’ of the Monkey* (Provincetown, MA: Journal Press)
- [2] Pribram K H 1971 *Languages of the Brain* (Engelwood Cliffs, NJ: Prentice-Hall)  
Pribram K H 1991 *Brain and Perception* (Hillsdale, NJ: Lawrence Erlbaum Associates Publ.)
- [3] Bach-y-Rita P 1995 *Nonsynaptic Diffusion Neurotransmission and Late Brain Reorganization* (New York: Demos-Vermande)
- [4] Bach-y-Rita P 2004 *Ann. N Y Acad. Sci.* **1013** 83  
Bach-y-Rita P 2005 *J. Integr. Neurosci.* **4** 183
- [5] Freeman W J 2005 *J. Integr. Neurosci.* **4** 407

- [6] Freeman W J 2006 *Clin. Neurophysiol.* **117** 572
- [7] Freeman W J and Vitiello G 2006 *Phys. Life Rev.* **3** 93 (Preprint q-bio.OT/0511037)
- [8] Freeman W J, Burke B C, Holmes M D and Vanhatalo S 2003 *Clin. Neurophysiol.* **114** 1055
- [9] Freeman W J, Burke B C and Holmes M D 2003 *Human Brain Mapp.* **19** 248
- [10] Freeman W J 2004 *Clin. Neurophysiol.* **115** 2077
- [11] Freeman W J 2004 *Clin. Neurophysiol.* **115** 2089
- [12] Freeman W J 2005 *Clin. Neurophysiol.* **116** 1118
- [13] Freeman W J, Gaál G and Jornten R 2003 *Intern. J. Bifurcation Chaos* **13** 2845
- [14] Freeman W J and Rogers L J 2003 *Intern. J. Bifurcation Chaos* **13** 2867
- [15] Bassett D S, Meyer-Lindenberg A, Achard S, Duke T and Bullmore E 2006 *PNAS* **103** 19518
- [16] Amit D J 1989 *Modeling Brain Function: The World of Attractor Neural Networks* (Cambridge: Cambridge University Press)
- [17] Morrow A L, Suzdak P D and Paul S M 1988 *Adv. Biochem. Psychopharmacol.* **45** 247
- [18] Schillen T B and König P 1994 *Biol. Cybern.* **70** 397
- [19] Roland P E 1993 *Brain Activation* (New York: Wiley-Liss)
- [20] Varela F, Lachaux J-P, Rodriguez E and Marinerie J 2002 *Nat. Rev. Neurosci.* **2** 229
- [21] Freeman W J 1975 *Mass Action in the Nervous System* (New York: Academic) (Reprinted 2004)
- [22] Terzuolo C A and Bullock T H 1961 *Proc. Natl Acad. Sci. USA* **42** 687
- [23] van Harrevelde A and Khattab F I 1968 *Anat. Rec.* **162** 467
- [24] Walker M M and Bitterman M E 1989 *J. Exp. Biol.* **145** 489
- [25] Azanza M J and del Moral A 1994 *Prog. Neurobiol.* **44** 517
- [26] Dunn J R, Fuller M, Zoeger J, Dobson J, Heller F, Hammann J, Caine E and Moskowitz B M 1995 *Brain Res. Bull.* **36** 149
- [27] Adey W R 1981 *Physiol. Rev.* **61** 435
- [28] Vitiello G 1995 *Int. J. Mod. Phys. B* **9** 973
- [29] Vitiello G 2001 *My Double Unveiled* (Amsterdam: John Benjamins)
- [30] Ricciardi L M and Umezawa H 1967 *Kibernetik* **4** 44
- [31] Stuart C I J, Takahashi Y and Umezawa H 1978 *J. Theor. Biol.* **71** 605  
Stuart C I J, Takahashi Y and Umezawa H 1979 *Found. Phys.* **9** 301
- [32] Sivakami S and Srinivasan V 1983 *J. Theor. Biol.* **102** 287
- [33] Umezawa H 1995 *Math. Jpn.* **41** 109
- [34] Del Giudice E, Doglia S, Milani M and Vitiello G 1985 *Nucl. Phys. B* **251** 375  
Del Giudice E, Doglia S, Milani M and Vitiello G 1986 *Nucl. Phys. B* **275** 185  
Del Giudice E, Preparata G and Vitiello G 1988 *Phys. Rev. Lett.* **61** 1085
- [35] Jibu M and Yasue K 1995 *Quantum Brain Dynamics and Consciousness* (Amsterdam: John Benjamins)  
Jibu M, Pribram K H and Yasue K 1996 *Int. J. Mod. Phys. B* **10** 1735
- [36] Celeghini E, Rasetti M and Vitiello G 1992 *Ann. Phys.* **215** 156
- [37] Alfinito E and Vitiello G 2000 *Int. J. Mod. Phys. B* **14** 853  
Alfinito E and Vitiello G 2000 *Int. J. Mod. Phys. B* **14** 1613 (erratum)
- [38] Umezawa H 1993 *Advanced Field Theory: Micro, Macro and Thermal Concepts* (New York: AIP)
- [39] Perelomov A 1986 *Generalized Coherent States and Their Applications* (Berlin: Springer)
- [40] Takahashi Y and Umezawa H 1975 *Collect. Phenom.* **2** 55  
Takahashi Y and Umezawa H 1996 *Int. J. Mod. Phys. B* **10** 1755 (reprinted)
- [41] Alfinito E, Romei O and Vitiello G 2002 *Mod. Phys. Lett. B* **16** 93
- [42] Alfinito E and Vitiello G 2002 *Phys. Rev. B* **65** 054105
- [43] Freeman W J and Vitiello G 2008 (in preparation)
- [44] Freeman W J, Rogers L J, Holmes M D and Silbergeld D L 2000 *J. Neurosci. Meth.* **95** 111
- [45] Freeman W J 2007 *Neurodynamics of Cognition and Consciousness* ed R Kozma and L Perlovsky (Berlin: Springer)
- [46] Haken H 1996 *Principles of Brain Functioning: A Synergetic Approach to Brain Activity, Behavior, and Cognition* (Berlin: Springer)  
Haken H 1999 *Analysis of Neurophysiological Brain Functioning* ed C Uhl (Berlin: Springer) p 7  
Haken H 2004 *Synergetics: Introduction and Advanced Topics* (Berlin: Springer)
- [47] Atmanspacher H and Scheingraber H 1990 *Can. J. Phys.* **68** 728
- [48] Pikovsky A, Rosenblum M and Kurths J 2001 *Synchronization—A Universal Concept in Non-linear Sciences* (Cambridge: Cambridge University Press)
- [49] Pessa E and Vitiello G 2003 *Mind Matter* **1** 59  
Pessa E and Vitiello G 2004 *Int. J. Mod. Phys. B* **18** 841

- [50] Srivastava Y N, Vitiello G and Widom A 1995 *Ann. Phys.* **238** 200  
Blasone M, Srivastava Y N, Vitiello G and Widom A 1998 *Ann. Phys.* **267** 61
- [51] Kelso J A S 1995 *Dynamic Patterns: The Self Organization of Brain and Behavior* (Cambridge: MIT Press)
- [52] Bressler S L 2002 *Curr. Dir. Psychol. Sci.* **11** 58
- [53] Fingelkurts A A and Fingelkurts A A 2004 *Int. J. Neurosci.* **114** 843
- [54] Linkenkaer-Hansen K, Nikouline V M, Palva J M and Iimonemi R J 2001 *J. Neurosci.* **15** 1370–7
- [55] Bak P 1996 *How Nature Works: The Science of Self-organized Criticality* (New York: Copernicus)
- [56] Jensen H J 1998 *Self-Organized Criticality: Emergent Complex Behavior in Physical and Biological Systems* (Cambridge: Cambridge University Press)
- [57] de Arcangelis L, Perrone-Capano C and Hermann H J 2006 *Phys. Rev. Lett.* **96** 028107
- [58] Novikov E, Novikov A, Shannahoff-Khalsa D, Schwartz B and Wright J 1997 *Phys. Rev. E* **56** R2387
- [59] Vitiello G 2004 *Int. J. Mod. Phys. B* **18** 785
- [60] Kelso J A S, Case P, Holroyd T, Horvath E, Raczaszek J, Tuller B and Ding M 1995 *Ambiguity in Mind and Nature* ed P Kruse and M Stadler (Berlin: Springer)
- [61] Eysenck M W 1994 *Principles of Cognitive Psychology* (Hillsdale, NJ: Lawrence Erlbaum)
- [62] Tsuda I 2001 *Behav. Brain Sci.* **24** 793
- [63] Skarda C A and Freeman W J 1987 *Brain Behav. Sci.* **10** 161
- [64] Fingelkurts A A and Fingelkurts A A 2001 *Brain and Mind* **2** 261
- [65] Bressler S L and Kelso J A S 2001 *Trends Cog. Sci.* **5** 26
- [66] Cohen L G *et al* 1997 *Nature* **389** 180
- [67] Von Melchner L, Pallas S L and Sur M 2000 *Nature* **404** 871
- [68] Merleau-Ponty M 1945 *Phenomenology of Perception* (C. Smith, Trans.) (New York: Humanities Press)
- [69] von Neumann J 1958 *The Computer and the Brain* (New Haven: Yale University Press)
- [70] Itzykson C and Zuber J 1980 *Quantum Field Theory* (New York: McGraw-Hill)
- [71] Anderson P W 1984 *Basic Notions of Condensed Matter Physics* (Menlo Park: Benjamin)
- [72] Marshak R E 1993 *Conceptual Foundations of Modern Particle Physics* (Singapore: World Scientific)
- [73] Bratteli O and Robinson D W 1979 *Operator Algebra and Quantum Statistical Mechanics* (Berlin: Springer)
- [74] von Neumann J 1955 *Mathematical foundations of Quantum Mechanics* (Princeton, NJ: Princeton University Press)
- [75] The dissipative quantum model is therefore different in a substantial way from brain models formulated in the Quantum Mechanics frame. For quantum mechanical brain models see Stapp H P 1993 *Mind, Matter and Quantum Mechanics* (Berlin: Springer)  
Stapp H P 2003 *Mind, Matter and Quantum Mechanics* (Berlin: Springer)  
Penrose R 1994 *Shadows of the Mind* (Oxford: Oxford University Press)  
Hameroff S and Penrose R 1996 *J. Conscious. Stud.* **3** 36
- [76] Goldstone J 1961 *Nuovo Cimento* **19** 154  
Goldstone J, Salam A and Weinberg S 1962 *Phys. Rev.* **127** 965
- [77] Higgs P 1966 *Phys. Rev.* **145** 1156  
Kibble T W B 1967 *Phys. Rev.* **155** 1554
- [78] For a study on the crossover from SBS condensation to the Bose–Einstein condensate (BEC) of pairs of fermionic atoms obtained in the laboratory, see for example Leggett A J 1980 *Modern Trends in the Theory of Condensed Matter* ed A Pekalski and R Przystawa (Berlin: Springer)
- [79] Wang X F and Chen G R 2003 *IEEE Trans. Circuits Syst.* **31** 6
- [80] Buxton R B 2001 *Introduction to Functional Magnetic Resonance Imaging: Principles and Techniques* (Cambridge: Cambridge University Press)
- [81] Freeman W J and Grajski K A 1987 *Behav. Neurosci.* **101** 766
- [82] Ohl F W, Scheich H and Freeman W J 2001 *Nature* **412** 733
- [83] Ohl F W, Scheich H and Freeman W J 2005 *The Auditory Cortex—A Synthesis of Human and Animal Research* ed X Knig, P Heil, E Budgeing and H Scheich (Mahwah, NJ: Lawrence Erlbaum) p 429